Available online at www.sciencedirect.com

ScienceDirect

journal homepage: www.elsevier.com/locate/issn/15375110

Research Paper

Spectral assessment of two-spotted spider mite damage levels in the leaves of greenhouse-grown pepper and bean

Ittai Herrmann [a], *Michael Berenstein* [a], *Tarin Paz-Kagan* [a], *Amit Sade* [b], *Arnon Karnieli* [a,*]

[a] *The Remote Sensing Laboratory, Ben-Gurion University of the Negev, Sede Boker Campus, 84990, Israel*
[b] *Bio-Bee Biological Systems Ltd, Sde Eliyahu, 10810, Israel*

ARTICLE INFO

Article history:
Received 23 August 2016
Received in revised form
19 February 2017
Accepted 23 February 2017

Keywords:
Spectral analysis
Partial least squares-discriminant analysis (PLS-DA)
Vegetation indices
Two-spotted spider mite
Integrated pest management

The two-spotted spider mite (*Tetranychus urticae* Koch; TSSM) feeds on the under-surface of leaves, piercing the chloroplast-containing cells and affecting pigments as well as leaf structure. This damage could be spectrally detectable in the visible and near-infrared spectral regions. The aim was to spectrally explore the ability to assess TSSM damage levels in greenhouse-grown pepper (*Capsicum annuum*) and bean (*Phaseolus vulgaris*) leaves. Several vegetation indices (VIs) provided the ability to classify early TSSM damage using a one-way analysis of variance. Hyperspectral (400–1000 nm) and multispectral (five common bands) data were analysed and cross-validated independently by partial least squares-discriminant analysis models. These analyses resulted in 100% and 95% success in identifying early damage with hyperspectral data reflected from pepper and bean leaves, respectively, and in 92% with multispectral data reflected from pepper leaves. Although the TSSM activity occurred on the underside of leaves their damage can be spectrally detected by reflected data from the upper side. Early TSSM damage identification to greenhouse pepper and bean leaves, that their sole damage was by TSSM, can be obtained by VIs, hyperspectral data, and multispectral data. This study shows that by using sub leaf spatial resolution early damage by TSSM can be spectrally detected. It can be potentially applied for greenhouses as well as fields as an early detection method for TSSM management.

1. Introduction

The two-spotted spider mite (*Tetranychus urticae* Koch; TSSM) feeds on various plants; currently 1110 host species have been reported worldwide outdoors as well as in greenhouses (Migeon & Dorkeld, 2015). Annual yield losses can be severe: 15% for strawberries in the USA, 14% for maize in France (Attia et al., 2013) and 20–45% for okra fruit in India (Kumar, Raghuraman, & Singh, 2015). To provide protection from solar ultraviolet light, to allow better web construction, and to protect itself from predators, the TSSM spends most of its time

* *Corresponding author*. Fax: +972 8 6596805.
E-mail addresses: ittai9@gmail.com (I. Herrmann), micbern@gmail.com (M. Berenstein), paztarin@gmail.com (T. Paz-Kagan), amits@biobee.com (A. Sade), karnieli@bgu.ac.il, karnieli@bgu.ac.il (A. Karnieli).
http://dx.doi.org/10.1016/j.biosystemseng.2017.02.008
1537-5110/

Nomenclature

ANOVA	analysis of variance
B	blue spectral region or band (490 nm)
G	green spectral region or band (560 nm)
GLSW	generalised least squares weighting
GNDVI	green normalised difference vegetation index
HD	high damage
LD	low damage
LVs	latent variables
MD	medium damage
ND	no damage
NDVI	normalised difference vegetation index
NIR	near-infrared spectral region or band (790 nm)
NRENDVI	near-infrared red-edge normalised difference vegetation index
PLS-DA	partial least squares-discriminant analysis
R	red spectral region or band (666 nm)
RE	red-edge spectral region or band (715 nm)
REBNDVI	red-edge blue normalised difference vegetation index
REGNDVI	red-edge green normalised difference vegetation index
REIP	red-edge inflection point
TCARI	transformed chlorophyll absorption reflectance index
TGI	triangular greenness index
TSSM	two spotted spider mite
VI	vegetation index
VIP	variable importance in projection
VIS	visible
ρ_i	reflectance, transmittance or absorbance in i wavelength (nm) or band

on the under-surface of leaves (Sakai & Osakabe, 2010) where, amongst other activities, it lays eggs and feeds. Feeding occurs by piercing the chloroplast-containing cells in the mesophyll layer (Fraulo, Cohen, & Liburd, 2009), thus decreasing the leaf chlorophyll content. Nihoul, Vanimpe, and Hance (1991) presented a positive exponential correlation between TSSM density and leaf damage, while Alatawi, Margolies, and Nechols (2007) found a correlation between cumulative TSSM density and leaf damage. The severity of the damage as inflicted by the amount and rate of change in leaf chlorophyll depends on TSSM density and duration of feeding (Alatawi et al., 2007) and the defensive reaction of the plant host (Kant, 2006). Leaf damage caused by TSSMs can be seen by the human eye and therefore can be potentially detected by spectral means in the visible (VIS; 400–700 nm) spectral region. The spectral data obtained from a leaf is influenced by the chemical, as well as the physical, properties of the leaf. The leaf spectrum is highly affected by pigmentation in the VIS region (Yoder & Pettigrew-Crosby, 1995; Zhao et al., 2014), while the near-infrared (NIR; 700–1000 nm) region is mainly influenced by the cell arrangement and density (Gausman, 1985; Karnieli et al., 2013). The red-edge (RE) region, located between the red and the NIR wavelengths of vegetation reflectance, is known to be sensitive to chlorophyll content (Curran, Dungan, & Gholz, 1990). TSSMs feed by piercing cell walls and consuming their content; through this process, they change the leaf chemical and physical properties, potentially allowing the identification of TSSM damage by the VIS and NIR spectral regions (Herrmann et al., 2012; Mirik et al., 2006; Reisig & Godfrey, 2007). Therefore, it was hypothesised that, under the optimal plant growth conditions that can be provided in greenhouses, spectral measurements of the upper surface of the leaves, in the range of 400–1000 nm, can lead to TSSM damage identification.

Previous studies have mainly explored the spectral relationship to the number of arthropods (Fitzgerald, Maas, & Detar, 2004; Mirik et al., 2006; Reisig & Godfrey, 2010; Yang, Rao, Elliott, Kindler, & Popham, 2009). Since TSSM are mobile and can move from leaf to leaf as well as to other plants the focus of the current study was on the damage level they inflict. Although it was not possible to find a unique spectral signature for TSSM or aphid stressed cotton at the leaf scale (Reisig & Godfrey, 2007), Yang et al. (2009) reported ability to separate between stress inflicted by greenbug (*Toxoptera graminum*) and the Russian wheat aphid (*Diuraphis noxia*) on wheat at the canopy scale using multispectral means. This separation ability was based on comparisons made for equal durations after infestation by both pests. There were no results presented or discussion regarding damage levels. If optimal growing conditions are available for plants in a greenhouse, the main stress sources to identify will be insects and diseases. Small-scale studies using close range devices for sub-leaf analysis are useful as a first step towards large-scale applications by ground, airborne, and even satellite-based sensors on the canopy or sub-field level (Reisig & Godfrey, 2007). Since TSSMs prefer young leaves (Nihoul et al., 1991) that are usually found at the outer part of the canopy, TSSM damaged leaves can potentially be identified by spectral devices with adequate spatial resolutions.

Specific bands or vegetation indices (VIs) sensitive to damage inflicted by a particular species of arthropods or stress have not yet been discovered (Fitzgerald et al., 2004; Mirik et al., 2006; Reisig & Godfrey, 2007; Yang et al., 2009). Lan, Zhang, Hoffmann, and Lopez (2013) research has determined four bands (550, 560, 680 and 740 nm) that are important for detecting the spectral differences among mite-infested cotton plants treated with various levels of miticide. They concluded that the amount of miticide used for spider mite control can be reduced, since applying a half dose of miticide resulted in the same spectral reflectance of infested cotton plants as the full portion. Spider mites can rapidly develop resistance to pesticides (Dekeyser, 2005); therefore, other control methods should be considered. Another method of pest control, mainly used in greenhouses, is to release their natural enemies in order to suppress the pests (Legowski, 1966). Nansen, Sidumo, Martini, Stefanova, and Roberts (2013) presented results that showed a negative relationship between potassium content in dry leaf matter and the attractiveness of maize leaves to mites. Since the relative reflectance of 740 nm was revealed to be significantly negatively correlated with potassium content, it was suggested that this reflectance could be used for pest infestation risk assessment.

It is essential to detect insect damage as early as possible in order to facilitate efficient corrective action (Fraulo et al., 2009; Yang et al., 2009). Identification of TSSM damage should be

based on a sub-leaf spatial resolution that is sufficient to spectrally identify the small areas on the upper leaf surface affected by TSSM feeding. Early identification of TSSM damage and implementation of treatment, according to need, should minimise the reduction in yield and the amount of the natural enemies to be purchased and released (Alatawi et al., 2007), thus allowing potentially higher profits for the growers.

The ability to separate TSSM damage levels of pepper leaves by six VIs, obtained from reflected spectral data in the laboratory, was reported in Herrmann et al. (2012). A partial least squares-discriminant analysis (PLS-DA) and VIs were applied to analyse the reflected data from the pepper leaves in order to identify early TSSM damage, as reported in Herrmann, Berenstein, Paz-Kagan, Sade, and Karnieli (2015). The current study utilised reflected, absorbed and transmitted spectral data from TSSM-damaged pepper leaves, as well as reflected data from TSSM-damaged bean leaves. The data were analysed by eight VIs, and both hyperspectral and multispectral data were classified by PLS-DA. The aim was to spectrally explore the ability to assess TSSM damage levels in greenhouse-grown pepper and bean leaves. The ability to assess TSSM damage levels was explored for: (1) vegetation indices; (2) hyperspectral continuous data; and (3) multispectral data. The current study was oriented toward spectrally assessing the damage levels of two crops under different experimental designs. Each of the two crops were grown in a separate site, under different conditions and spectral measuring techniques, with different pest control advisors assessing the TSSM damage levels to the leaves. Thus, each crop dataset was analysed separately, and no claim is made here to compare the results for the crops but only to show the spectral abilities to analyse TSSM damage. Both pepper and bean spectral data were analysed by the same methods.

2. Material and methods

2.1. Study area and leaf collection

2.1.1. Pepper leaf collection

On January 4, 2010, in a commercial greenhouse in the northwest Negev Desert, Israel (31° 20′ N; 34° 24′ E), leaves from the outer and upper canopy of six-month-old pepper (*Capsicum annuum*) plants with four various TSSM damage levels were identified by a pest control advisor. Each leaf was from a different plant. The leaves were classified into damage levels and marked, resulting in 97 leaves. After they were all marked, they were collected, put into plastic bags inside a thermally isolated case and cooled by ice, with no direct contact with the leaves or the bags. As presented by Herrmann et al. (2012), the pepper leaves were categorised into four TSSM damage levels: no damage (ND; 25 samples); low damage (LD; 26 sample); medium damage (MD; 23 samples); and high damage (HD; 23 samples), as can be seen in Fig. 1. The leaves were transported to the laboratory for spectral measurements that took place within 4 h of leaving the greenhouse.

2.1.2. Bean leaf collection

On March 10, 2013, in a BioBee Ltd greenhouse in the Jordan Valley, Israel (32° 26′ N; 35° 30′ E), leaves from the outer and upper canopy of 40-day old bean (*Phaseolus vulgaris*) plants were examined, 25 d after the greenhouse was infested with TSSM as part of the process of producing a predator product to which to apply biological TSSM management. The leaves had various TSSM damage levels and were classified by a pest control advisor into four damage levels: ND (23 samples); LD (27 samples); MD (27 samples); and HD (27 samples), as can be seen in Fig. 1. Leaves were picked and placed in a cooled container; as many as 15 min elapsed between picking the leaves and obtaining the spectral measurements. Each leaf was picked from a different plant.

2.2. Spectral data collection

Spectral data were obtained by an ASD spectroradiometer FieldSpec Pro FR (Analytical Spectral Devices, Inc., Boulder, CO, USA) with a range of 350–2500 nm. The spectroradiometer was programmed to average 40 readings for each measurement, dark current as well as white reference. The dark current was applied automatically by the spectroradiometer as it was optimised for the lighting conditions facing the white reference barium sulphate ($BaSO_4$) surface. The white reference measurement allowed an output in relative units by dividing each measurement by the last acquired white reference measurement. It was applied to minimise the influence of drift in the system (i.e., light source, as well as detector). The spectral output of the spectroradiometer was in relative units with 1 nm intervals.

2.2.1. Spectral data collection of pepper leaves

The spectral measurements were obtained at the Remote Sensing Laboratory at the Jacob Blaustein Institutes for Desert Research, Sede Boker Campus, Ben-Gurion University, Israel. To apply reflectance and transmittance measurements, for each leaf, an external integrating sphere 1800-12s (LI-COR, Inc., Lincoln, NE, USA) was connected to the fibre optic of the ASD spectroradiometer. The light source of the integrating sphere was a tungsten halogen bulb. The leaf was placed in the sample clip with its upper side facing the inner part of the integrating sphere. To obtain a white reference, as well as to measure reflectance from a leaf, both the light source and the fibre optic directly faced the inner part of the sphere and never each other, as presented in Fig. 2. The inner part of the sphere was coated with barium sulphate ($BaSO_4$). Figure 2 presents the system configuration for transmittance leaf measurements, the light source was relocated to illuminate through the leaf, with the fibre optic still directly facing the inner part of the sphere. The leaf reflectance and transmittance measurements of each leaf were obtained while the leaf was kept in place.

2.2.2. Spectral data collection of bean leaves

The reflectance spectral measurements were obtained in the greenhouse. The measurements were made in contact with the leaf, and the fibre optic of the ASD spectroradiometer was connected to a contact probe (Analytical Spectral Devices, Inc., Boulder, CO, USA) equipped with tungsten halogen bulb. Each leaf was placed on a black background with its upper side surface facing up. The contact probe was placed by hand to touch, but not press, the leaf for each measurement. To obtain a white reference, a barium sulphate ($BaSO_4$) panel was used.

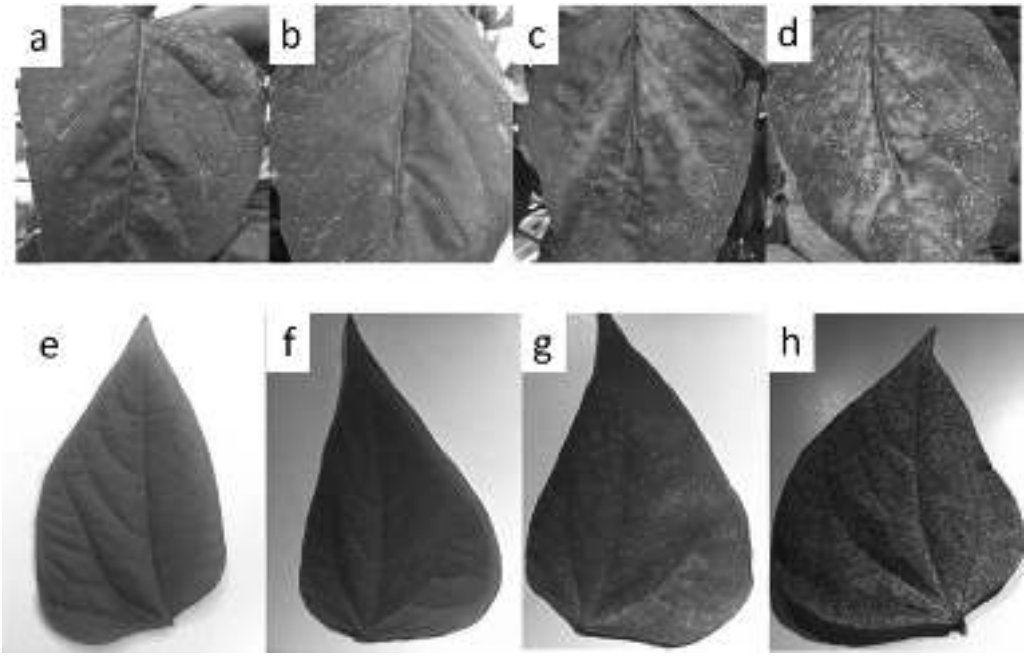

Fig. 1 – The four damage levels as visually observed on the adaxial surface of pepper and bean leaves. Pepper leaves: (a) no damage (ND); (b) low damage (LD); (c) medium damage (MD); (d) high damage (HD). Bean leaves: (e) no damage (ND); (f) low damage (LD); (g) medium damage (MD); (h) high damage (HD). The amount of two-spotted spider mites (TSSMs) on the under-surface of the leaf does not represent the severity of the damage.

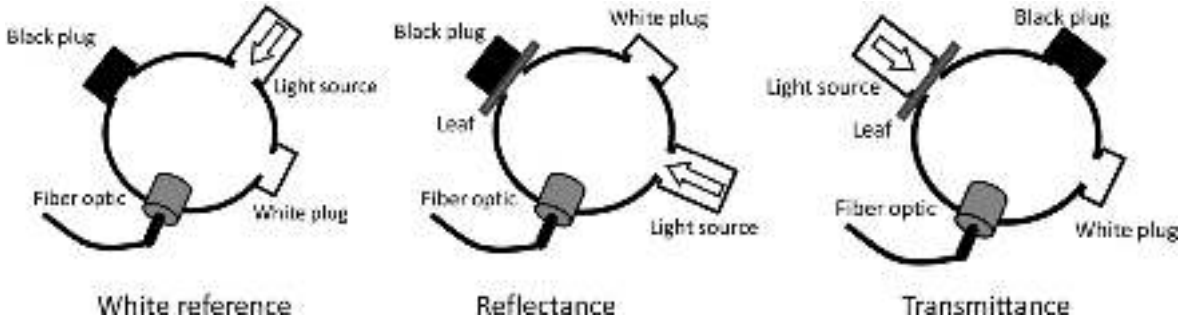

Fig. 2 – The three configurations used by the 1800-12s integrating sphere (LI-COR, Inc., Lincoln, NE, USA): white reference, obtaining the 100% radiation available by the system; reflectance, obtaining the radiation reflected form leaf sample; and transmittance, obtaining the radiation transmitted via leaf sample. It was assumed that since the sphere is sealed the light source was the only source of radiation. When using the white reference there was no leaf sample in the sample port. To keep the reflective area of the inner surface of the integrated sphere constant for all configurations a black plug is placed in the sample port. Therefore, these three configurations keep the same area of the inner surface of the integrating sphere. The black plug and light source were never included in the field of view of the fibre optic. This figure is based on the LI-1800 portable spectroradiometer instruction manual (LI-COR, 1989) that the 1800-12s integrating sphere is one of its accessories.

The reference panel was prepared by pressing and smoothing, with glass, the powder into a container that fit the diameter of the contact probe to allow maximal reflectance from a smooth surface. The white reference measurements were obtained every 10 min.

2.3. *Data analyses*

The spectral data of both the pepper and bean leaves were resampled to 2 nm intervals for the range of 400–1000 nm. In order to obtain the relative absorbance spectra of the pepper leaves, the relative reflectance and relative transmittance spectra of specific samples were subtracted from a vector with the same length that contained only the value 1 (100%), based on the fact that the balance of electromagnetic radiation that illuminates a leaf is divided between reflectance, absorption, and transmittance (Jacquemoud & Baret, 1990). Table 1 presents broad bands obtained by averaging continuous spectra in the specified ranges. The blue (B), green (G), and red (R) bands are available in the majority of the commercial digital

Table 1 – Ranges and centres of the resampled multispectral bands. The intensity value of the band was obtained by averaging the intensity of wavelengths included in the range of the band.

Band	Centre (nm)	Range (nm)
Blue (B)	490	470–510
Green (G)	560	540–580
Red (R)	666	656–676
Red-edge (RE)	715	710–720
Near-infrared (NIR)	790	770–810

cameras and applied in the areas of crop traits, relative coverage, and stress detection (Karnieli et al., 1996; Mirik et al., 2006). Commercial cameras can be converted to include NIR data by several methods. The RE band is rarely used in commercial digital cameras (Hunt et al., 2010). Broad bands were used to obtain the VIs presented in Table 2. The broad band VIs include the normalised difference vegetation index (NDVI; Rouse, Haas, Schell, & Deering, 1973), the green NDVI (GNDVI; Gitelson, Kaufman, & Merzlyak, 1996), the red-edge GNDVI (REGNDVI; Herrmann et al., 2012), the red-edge blue NDVI (REBNDVI; Herrmann et al., 2012), and the near-infrared red-edge NDVI (NRENDVI; Herrmann et al., 2012). The triangular greenness index (TGI; Hunt, Daughtry, Eitel, & Long, 2011) was calculated by a combination of broad bands and the centres of the R, G, and B bands. Also presented are narrow band VIs that were calculated by narrow bands from the spectral data. The narrow bands VIs: the transformed chlorophyll absorption reflectance index (TCARI; Haboudane, Miller, Tremblay, Zarco-Tejada, & Dextraze, 2002) and the red-edge inflection point (REIP; Guyot & Baret, 1988). All VIs were calculated for the reflectance, absorbance, and transmittance spectra of pepper leaves and the reflectance of bean leaves. A one-way analysis of variance (ANOVA) was applied in order to determine whether a VI can provide significant separation between damage levels. The ANOVA was applied for each of the indices for all possible couplings of damage levels. It was executed by Matlab 7.6 (MathWorks, Natick, MA, USA).

The PLS-DA is a PLS model applied to the discriminant function analysis problem in order to allow maximal separation among predefined classes (Musumarra, Barresi, Condorelli, Fortuna, & Scire, 2004). To combine the PLS (numerical) and the DA (categorical), each class was assigned a binary artificial sequence of arbitrary numbers. This sequence was assigned to all the class samples. The size of the sequence was set by the number of classes to classify (Musumarra et al., 2004). The PLS-DA models were applied in a Matlab 7.6 environment by the PLS-toolbox (Eigenvector, Wenatchee, WA, USA). Pre-processing transformations can improve the classification accuracy by increasing the variability between classes while decreasing variability within them (Rozenstein, Paz-Kagan, Salbach, & Karnieli, 2015). Therefore, prior to building the PLS-DA models, the spectral data were pre-processed by two transformations: (1) generalised least squares weighting (GLSW) that down weighted the differences between samples of the same class (Paz-Kagan, Shachak, Zaady, & Karnieli, 2014); and (2) mean centring that was applied as pre-processing for PLS models by calculating the mean of each wavelength and subtracting it from each intensity value of the wavelength for all samples (Navalon, Blanc, del Olmo, & Vilchez, 1999). This combination of transformations was chosen based on Rozenstein et al. (2015) findings as well as trial and error to obtain the best classification model. The cross-validation method used was venetian blinds with 10 splits. PLS-DA models for separation between the four damage levels were built for the reflectance, absorbance, and transmittance spectra of pepper leaves and the reflectance of bean leaves. Each model resulted in a confusion matrix that described the ability to correctly classify each of the classes, as well as the overall accuracy of the classification. The quality of the classification was assessed by Cohen's Kappa coefficient (Cohen, 1960), the overall accuracy with confidence limit (Foody, 2008), user accuracy, and producer accuracy for each of the confusion matrices.

The hyperspectral data, of both pepper and bean, were resampled to the bands presented in Table 1. PLS-DA models were applied for reflectance, absorbance, and transmittance, hereafter denoted measuring methods, of pepper leaves and the reflectance of bean leaves. For each of the multispectral models, the variable importance in projection (VIP) was obtained. The VIP is defined as the weighted sum of the importance of each wavelength in all projections of the PLS model (Wold, Johansson, & Cocchi, 1993). The VIP values are

Table 2 – Equations and types of indices. For the broad bands, ρ stands for the relative reflectance, transmittance, or absorbance value of the subscripted broad band as specified in Table 1. In the case of the triangular greenness index (TGI), the stand-alone capital letters represent the centre of the broad band as specified in Table 1. For the narrow bands, ρ stands for the relative reflectance, transmittance, or absorbance value of the subscripted number in nm.

Indices	Index type	References
$NDVI = \frac{\rho_{NIR}-\rho_R}{\rho_{NIR}+\rho_R}$	Broad band	Rouse et al. (1973)
$GNDVI = \frac{\rho_{NIR}-\rho_G}{\rho_{NIR}+\rho_G}$	Broad band	Gitelson et al. (1996)
$REGNDVI = \frac{\rho_{RE}-\rho_G}{\rho_{RE}+\rho_G}$	Broad band	Herrmann et al. (2012)
$REBNDVI = \frac{\rho_{RE}-\rho_B}{\rho_{RE}+\rho_B}$	Broad band	Herrmann et al. (2012)
$NRENDVI = \frac{\rho_{NIR}-\rho_{RE}}{\rho_{NIR}+\rho_{RE}}$	Broad band	Herrmann et al. (2012)
$REIP = 700 + 40\left\{\frac{[(\rho_{670}+\rho_{780})/2]-\rho_{700}}{\rho_{740}-\rho_{700}}\right\}$	Narrow band (inflection point)	Guyot and Baret (1988)
$TCARI = 3\left[(\rho_{700}-\rho_{670})-0.2(\rho_{700}-\rho_{550})\left(\frac{\rho_{700}}{\rho_{670}}\right)\right]$	Narrow band	Haboudane et al. (2002)
$TGI = -0.5[(R-B)(\rho_R-\rho_G)-(R-G)(\rho_R-\rho_B)]$	Broad band (area)	Hunt et al. (2011)

evaluated by "the higher the better" method with a threshold of one (Cohen et al., 2010). The hyperspectral and multispectral confusion matrices were coupled in order to check whether they were significantly different. The method of obtaining this information was based on Cohen's Kappa and the variance of the matrix as detailed by Herrmann, Shapira, Kinast, Karnieli, and Bonfil (2013).

3. Results and discussion

The spectral averages for each of the four damage levels of the pepper leaves with the three measuring techniques are shown in Fig. 3a–c, respectively. As seen in Fig. 3b, around 800 nm, the relative absorbance values of the four damage levels increased with increasing damage level, from ND to HD. However, the absorbance values and damage levels were negatively related around 600 nm. The spectra are ordered by either the increasing or decreasing severity of the damage level. However, there are cases where not all the spectra are ordered by the severity of damage level. In Fig. 3a, around 670 nm, it can be seen that the relative reflectance values of ND, LD and MD increased, respectively, while the HD spectrum shifted the trend. Around 670 nm, there was a chlorophyll absorption trough (Haboudane et al., 2002; Tucker, 1979). Therefore, since chlorophyll was consumed by TSSMs, it was expected that the HD spectrum would keep the increasing trend in reflectance by damage level. Since it did not behave in the expected manner, it was thought that the other measuring techniques might shed some light on the reason. Figure 3b shows a decrease in relative absorbance as the damage severity increases, while Fig. 3c shows an increase in relative transmittance as the damage level increases. Therefore, it was assumed that in the HD level, the chlorophyll level was reduced and the absorbance decreased. Similar to the 670 nm region, the region of 400–500 nm in Fig. 3a was affected by chlorophyll and beta carotene (Jacquemoud & Baret, 1990). In this range, the decrease in the reflectance spectrum of leaves damaged by arthropods agreed with the results of Fitzgerald et al. (2004) for cotton but not with those of Mirik et al. (2006) for winter wheat. Both pepper and cotton are dicotyledonous, while wheat is monocotyledonous; therefore, beyond any species difference, there was an inherent difference in leaf structure (Raven, Everet, & Eichhorn, 2005). Since the TSSMs destroy cells while eating, the leaf loses biomass and becomes more transparent for

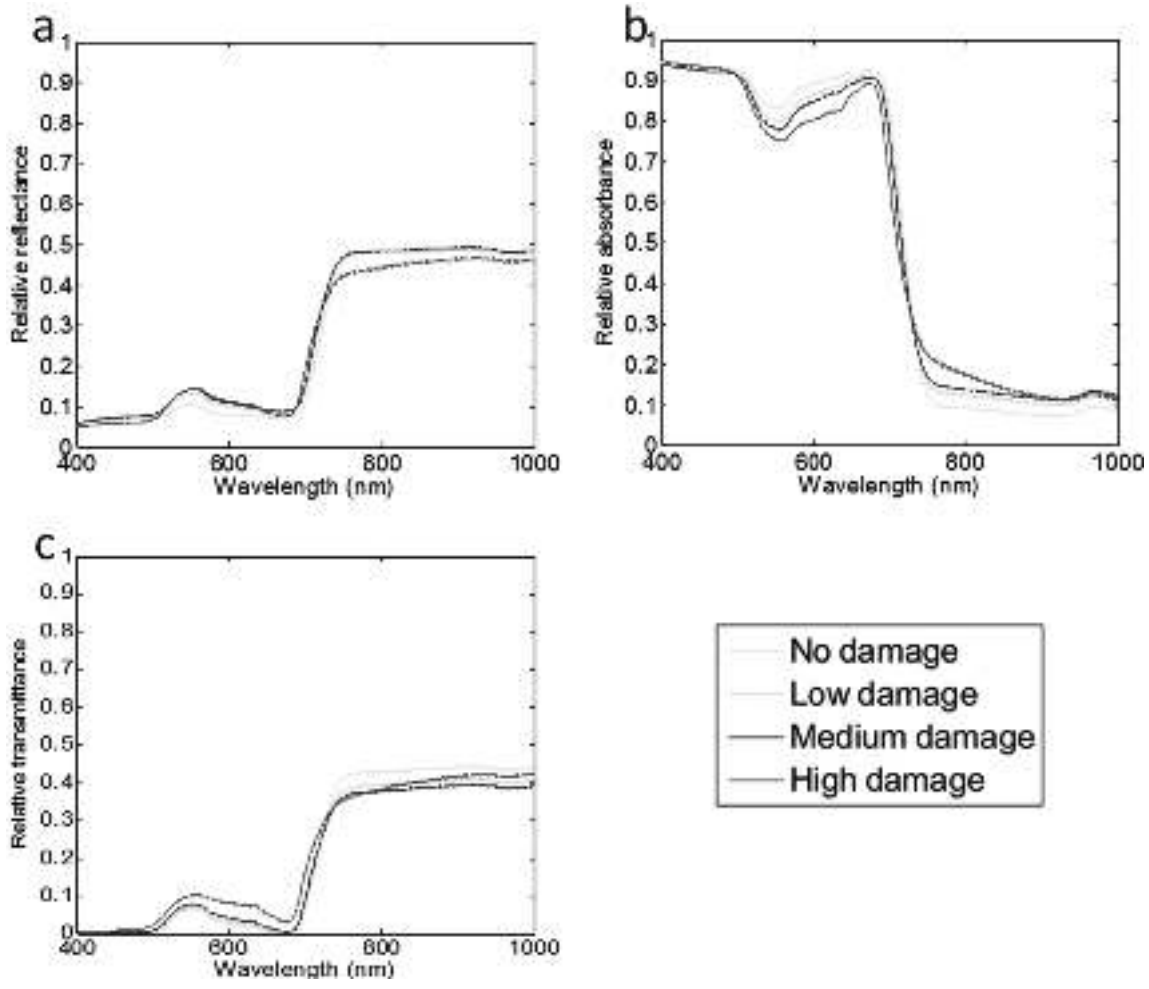

Fig. 3 – Averaged spectra for each of the four damage levels. (a) reflected from leaf; (b) absorbed in leaf; and (c) transmitted through pepper leaves. The ± standard error lines are so close to the average lines that they are not distinct.

visible light. The increase in transparency in the visible spectral region can be seen in Fig. 3c. The inner leaf structure causes the increased reflectance in the NIR region (Gausman, 1985). Since the inner leaf structure was damaged, there was a decrease in the NIR region's reflectance. In this region, the severity of the damage was negatively related to transmission and positively related to absorption. In the case of transmission, the spectral response in the NIR region were ordered by severity (high intensity for low damage level) three damage levels while the HD behaved differently, assuming it to be influenced by leaf thickness and structure (Kiang, Siefert, Govindjee, & Blankenship, 2007). There were spectral differences between the damage levels measured by the three different methods. These spectra were assessed for their ability to separate between damage levels by VIs for specific band combinations, as well as by PLS-DA for the entire spectrum. Figure 4 presents the spectral average for bean leaves for the four damage levels. The ND, LD and MD are very similar, and the HD reflects the most in all wavelengths, showing that less was absorbed by the chlorophyll, resulting in a blue shift that is defined as the movement of the red-edge inflection point to shorter wavelengths as a result of changes in biological and/or biophysical leaf traits (Mutanga & Skidmore, 2007). The blue shift relationship to increasing damage agrees with the findings of Nansen et al. (2013), showing a positive relationship between the relative reflectance in 740 nm and the attractiveness of maize leaves to mites. In the current study, the stress was the TSSM damage that decreased the chlorophyll content, as well as harmed the leaf structure. The differences in the spectral data of the four damage levels of the two crops can be related to: differences in leaf inner structure; availability of the same damage levels; different environmental conditions and experimental designs; and damage patterns. The pepper had homogeneous areas of damage as presented in (Herrmann et al., 2012) as well as Fig. 1, while the bean, as also shown in the figure, showed white damage in a spotty pattern.

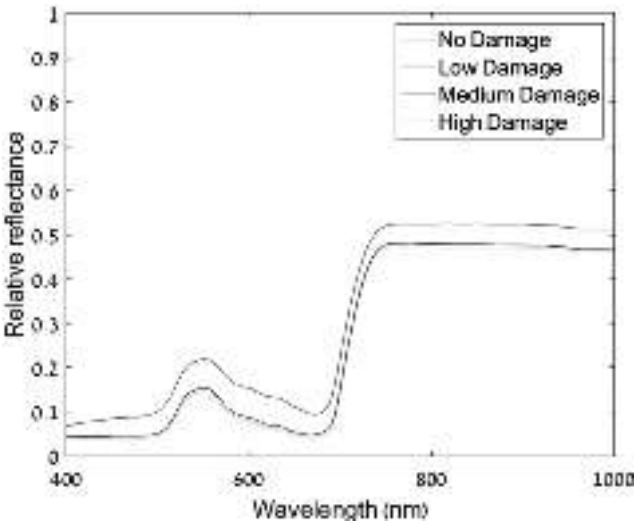

Fig. 4 – Averaged spectra for each of the four damage levels reflected from bean leaves. The ± standard error lines are so close to the average lines that they are not distinguishable.

3.1. *Vegetation indices*

3.1.1. *Separating two spotted spider mite damage level to pepper leaves by vegetation indices*

Table 3 presents the damage level separation by ANOVA based on pepper VI values for reflectance, absorbance, and transmittance. Different letters represent the ability to significantly differentiate between coupled damage levels, whereas the same letter represents coupled damage levels that are not significantly different based on the VI values. For the reflectance measurements, there were two indices that separated all four damage levels for the $p < 0.01$ significance: TCARI and TGI. In the case of the $p < 0.05$ significance, three indices were added. For the absorbance measurements, there were three indices that separated all four damage levels for the $p < 0.01$ significance: NRENDVI, REIP, and TGI. In the case of the $p < 0.05$ significance, two were added. For the transmittance data, only the REIP separated all four damage levels for the $p < 0.01$ significance. In the case of the $p < 0.05$ significance, three were added. The VIs that showed significance, for the three measuring methods, in separating the four damage levels were NRENDVI and REIP. The latter was slightly better

Table 3 – The ability of each index, obtained by reflected, absorbed and transmitted data from pepper leaves, to separate between damage levels by one-way ANOVA. Different letters stand for the ability to significantly separate between coupled damage levels, whereas the same letter stands for coupled damage levels that are not significantly different. The small letters are for $p < 0.01$, and the capital letters are for $0.01 < p < 0.05$. In cases for which there are no capital letters, the $0.01 < p < 0.05$ the ability to separate is the same as for $p < 0.01$.

	No damage	Low damage	Medium damage	High damage
Reflectance				
NDVI	a	a, b	b	b
GNDVI	a	b	b	c
REGNDVI	a, c	a, b	b	b, c
REBNDVI	a	a, b	b	c
NRENDVI	a [A]	b [B]	b [C]	c [D]
REIP	a [A]	b [B]	b [C]	c [D]
TCARI	a	b	c	d
TGI	a	b	c	d
Absorption				
NDVI	a	b	b	c
GNDVI	a [A]	b [B]	b [C]	d [D]
REGNDVI	a	b	b	c
REBNDVI	a	b	b	c
NRENDVI	a	b	c	d
REIP	a	b	c	d
TCARI	a [A]	b [B]	b [C]	c [D]
TGI	a	b	c	d
Transmittance				
NDVI	a [A]	b [B]	b [C]	c [D]
GNDVI	a [A]	b [B]	b [C]	c [D]
REGNDVI	a [A]	a, d [B]	b, d [B]	c [C]
REBNDVI	a [A]	a [B]	a [B]	b [D]
NRENDVI	a [A]	b [B]	b [C]	c [D]
REIP	a	b	c	d
TCARI	a, b, c [A, C]	a, b, c [A, B]	b [B]	c [C]
TGI	a [A]	a [B, C]	a, b [C, D]	b [D]

since it had a higher level of significance, $p < 0.05$ for reflectance and $p < 0.01$ for the other two measuring methods. In the matter of separating only the ND damage level, the reflectance data showed five indices with $p < 0.1$ significance. The absorbance measurements showed that all VIs could identify the ND damage level with $p < 0.1$ significance. The transmittance data showed that four had $p < 0.01$ significance. In the case of those with $p < 0.05$ significance, three VIs were added. The indices that showed significance in the separation of ND from LD damage levels were GNDVI, NRENDVI, REIP and TGI. Since the LD and MD are the damage levels that have the lowest separation rates in Table 3, it can be assumed that the intermediate damage levels are more difficult to identify than the ND and HD damage levels. Since GNDVI, NRENDVI, REIP, and TGI can separate between ND and the damage levels with actual damage (i.e., LD, MD, and HD), they are potentially applicable for site-specific TSSM damage identification.

3.1.2. *Separating two spotted spider mite damage level to bean leaves by vegetation indices*

Table 4 presents the damage level separation by ANOVA based on VI values calculated from reflectance of bean leaves. Only the NDVI could separate between the four damage levels. However, the rest of the indices, with the exception of GNDVI, could separate the HD level from the other three damage levels. Identification of HD by TSSMs might occur too late to control (Alatawi et al., 2007) since in order to get to the stage of HD, a certain amount of time must pass, allowing the TSSMs to spread and inflict damage to other plants. It is important to mention that the mite damage and healthy leaf spectral signatures presented by Fitzgerald et al. (2004), Mirik et al. (2006), and Lan et al. (2013) seemed to show relatively larger spectral changes in the VIS and NIR regions than those presented in the current study between ND and HD. Therefore, it was assumed that the definition of HD damage level in the current study represents less damage compared to the arthropod damage presented in the other studies, as shown in their figures of spectral reflectance.

Table 4 – The ability of each index, obtained by reflected data from bean leaves, to separate between damage levels by one-way ANOVA. Distinct letters stand for the ability to significantly separate between coupled damage levels, whereas the same letter stands for coupled damage levels that are not significantly different. The small letters are for $p < 0.01$, and the capital letters are for $0.01 < p < 0.05$. In cases in which there are no capital letters, the $0.01 < p < 0.05$ the ability to separate is the same as for $p < 0.01$.

	No damage	Low damage	Medium damage	High damage
NDVI	a	b	c	d
GNDVI	a [A, C]	a [A]	a [A, C]	b [B]
REGNDVI	a [A]	a, d [A]	b, d [B]	c [C]
REBNDVI	a	b	b	c
NRENDVI	a	a	a	b
REIP	a	a	a	b
TCARI	a	a	a	b
TGI	a	a	a	b

3.2. *Partial least squares-discriminant analysis*

3.2.1. *Separating two spotted spider mite damage level to pepper leaves by partial least squares –discriminant analysis*

The PLS-DA cross-validation hyperspectral models of the three measuring methods for pepper leaves were optimised by three latent variables (LVs). The scores are the coefficients of each of the samples in a specific projection that was defined as LV. The scores of each of the classes (damage levels) for the three possible couplings of LVs are presented in Fig. 5. The scores are segregated by classes. Since the PLS-DA classification is linear, these cases might not be perfectly classified. The classification results for the four damage levels by the entire spectra, reflected, absorbed, and transmitted, are presented in Table 5. The overall accuracy of the three measuring methods resulted in 83.5%, 82.5%, and 82.5%, respectively. The confidence intervals and the Cohen's Kappa also contained minor differences. Therefore, the differences in overall accuracies and the Cohen's Kappa were assumed to be negligible. There were no dramatic differences between the accuracies of the classes for the three measuring methods. Consequently, in the case discussed, applying reflectance was considered to be as equally advantageous as transmittance. The ND was perfectly classified for the three measuring methods. Therefore, early detection of TSSM damage, by hyperspectral data reflected from pepper leaves, is potentially applicable.

The hyperspectral data, obtained from pepper leaves, were resampled to the multispectral bands presented in Table 1 in order to explore the multispectral classification by PLS-DA models. The reflectance and transmittance models had the same pre-processing parameters as the hyperspectral models, while the absorbance model gave better results with no pre-processing. They also resulted in three LVs, and the scores of the reflectance, absorbance and transmittance models are presented in Fig. 6. The plotted scores presented are the result of rotating the axes to look for the best separation by eye. The distribution of the scores agrees with the confusion matrices presented in Table 7. The hyperspectral and multispectral confusion matrices of each of the measuring methods were coupled to check whether they were significantly different. The results indicated that the reflectance data were not significantly different $p > 0.05$, while the other two pairs showed significant differences $0.01 < p < 0.05$. Therefore, for reflectance, the multispectral model was as good as the hyperspectral model. Figure 7 presents the VIP of the PLS-DA multispectral models. In the case of the reflectance model, Fig. 7a, for the ND and HD classes, the RE band was the most influential band, while for the LD and MD classes, the G and R bands were the most influential. For all four damage levels, the NIR was above the threshold, and the B band was below it. This similarity between the LD and MD damage levels agrees with Table 6 showing that most of the misclassifications for these two classes were among themselves. As seen in Fig. 7b, the most influential bands for the four damage levels were RE and NIR. In Fig. 6c, again there are presented two pairs of damage levels. As seen in all sub-figures of Fig. 5, B band was below the threshold.

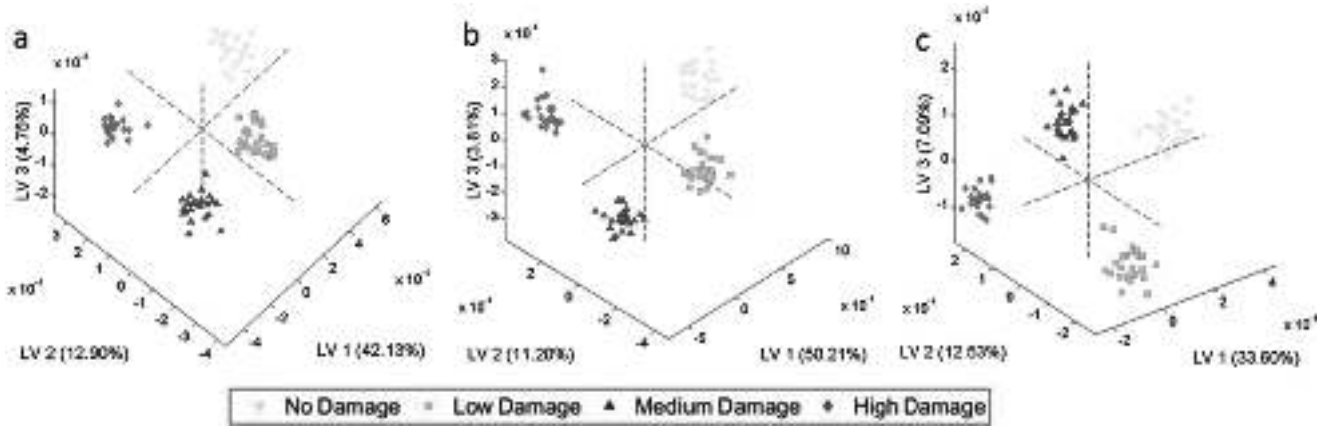

Fig. 5 – Scores of the PLS-DA cross-validation hyperspectral models, for pepper leaves, in three latent variables (LVs): (a) reflectance; (b) absorbance; and (c) transmittance. In the parentheses, the variances captured by the LVs are presented.

Table 5 – Cross-validation of the PLS-DA classification models of four damage levels based on the hyperspectral reflectance, absorbance and transmittance from pepper leaves. Each of the models is the result of three latent variables.

	No damage	Low damage	Medium damage	High damage	Total predicted as	User accuracy % correct
Reflectance						
Confidence limit of ±7.5% for the overall accuracy, and Kappa = 0.77						
No damage	**25**	0	0	0	25	100
Low damage	0	**24**	8	1	33	72.7
Medium damage	0	2	**14**	4	20	70
High damage	0	0	1	**18**	19	94.7
Total actual class	25	26	23	23	97	
Producer accuracy % correct	100	92.3	60.9	78.3		**83.5**
Absorbance						
Confidence interval of ±7.6% for the overall accuracy, and Kappa = 0.76						
No damage	**25**	0	0	0	25	100
Low damage	0	**24**	4	0	28	85.7
Medium damage	0	2	**14**	6	22	63.6
High damage	0	0	5	**17**	22	77.3
Total actual class	25	26	23	23	97	
Producer accuracy % correct	100	92.3	60.9	73.9		**82.5**
Transmittance						
Confidence interval of ±7.6% for the overall accuracy, and Kappa = 0.76						
No damage	**25**	0	0	0	25	100
Low damage	0	**25**	5	3	33	75.8
Medium damage	0	1	**16**	6	23	69.6
High damage	0	0	2	**14**	16	87.5
Total actual class	25	26	23	23	97	
Producer accuracy % correct	100	96.2	69.6	60.9		**82.5**

The bold values in the diagonal are the actual number of samples correctly classified and the bold value at the lower right corner of each sub table is the total accuracy in percentage.

3.2.2. *Separating two spotted spider mite damage level to bean leaves by partial least squares – discriminant analysis*

The PLS-DA cross-validation hyperspectral model of the reflectance from bean leaves was optimised by three LVs, and the multispectral model was optimised for four LVs. The hyperspectral model resulted in high classification quality with an overall accuracy of 94.2% and more than 88% for each of the classes. The multispectral model resulted in lower classification quality with an overall accuracy of 67.3%. The confusion matrices presenting the classification results of the hyperspectral and multispectral models are presented in Table 7, and the scores are presented in Fig. 8a and b, respectively. The hyperspectral and multispectral confusion matrices of the PLS-DA models for bean leaves were checked to determine whether they were significantly different. The results indicated that the classification results were significantly different $p < 0.01$. Therefore, there was an advantage to the hyperspectral classification quality for all TSSM damage levels. In the case of the HD level, the classification qualities (i.e., user and producer accuracies) were relatively high (above 93%) for both the hyperspectral and the multispectral models; thus, the ability to assess HD level by the multispectral model

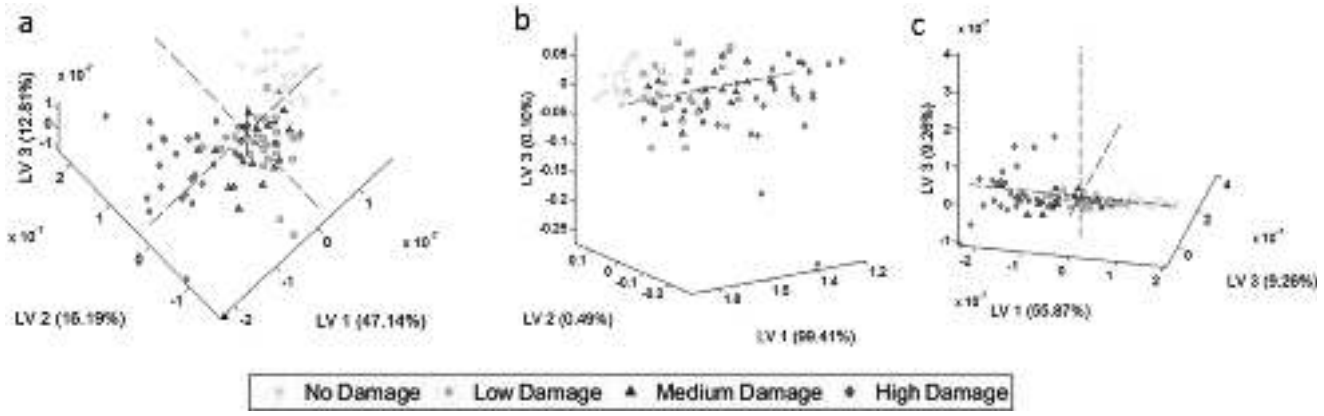

Fig. 6 – Scores of the PLS-DA cross-validation multispectral models, for pepper leaves, in three latent variables (LVs): (a) reflectance; (b) absorbance; and (c) transmittance. In the parentheses, the variances captured by the LVs are presented.

Table 6 – Cross-validation of the PLS-DA classification models of four damage levels based on the resampled multispectral reflectance, absorbance and transmittance from pepper leaves. Each of the models is the result of three latent variables.

	No damage	Low damage	Medium damage	High damage	Total predicted as	User accuracy % correct
Reflectance						
Confidence limit of ±8.9% for the overall accuracy, and Kappa = 0.64						
No damage	**24**	1	1	0	26	92.3
Low damage	1	**16**	7	1	25	64
Medium damage	0	5	**11**	2	18	61.1
High damage	0	4	4	**20**	28	71.4
Total actual class	25	26	23	23	97	
Producer accuracy % correct	96	61.5	47.8	86.9		**73.1**
Absorbance						
Confidence interval of ±9.2% for the overall accuracy, and Kappa = 0.60						
No damage	**24**	4	0	0	28	85.7
Low damage	1	**16**	11	1	29	55.1
Medium Damage	0	5	**8**	2	15	53.3
High damage	0	1	4	**20**	25	80
Total actual class	25	26	23	23	97	
Producer accuracy % correct	96	61.5	34.7	86.9		**70.1**
Transmittance						
Confidence interval of ±11% for the overall accuracy, and Kappa = 0.59						
No damage	**22**	5	0	0	27	81.4
Low damage	3	**16**	10	0	29	55.1
Medium damage	0	5	**10**	4	19	52.6
High damage	0	0	3	**19**	22	86.3
Total actual class	25	26	23	23	97	
Producer accuracy % correct	88	61.5	43.4	82.6		**69**

The bold values in the diagonal are the actual number of samples correctly classified and the bold value at the lower right corner of each sub table is the total accuracy in percentage.

was as good as by the hyperspectral model. Figure 8c shows the VIP of the multispectral PLS-DA model for classifying bean leaves. The HD line connecting the VIP values for the five bands was almost horizontal, showing no band that was much more important than the others. The VIS region was above the threshold; this suggests that most of the ability to assess HD level was based on chlorophyll content. This agrees with the spectral curve presented in Fig. 4 showing the HD curve to be very different from the other three damage levels.

The spectral data for bean was collected 25 d after infestation, and the PLS-DA analysis resulted in identifying HD. The spectral data for pepper were obtained at an unknown duration after the appearance of TSSMs in the greenhouse, and the PLS-DA analysis resulted in the ability to identify ND. It was tempting to solely relate the ability to identify ND to the duration of time since TSSM appearance. Using this relationship would neglect the biophysical differences between the two crops, as well as the different experimental designs. Therefore, measurement technique in relation to the targeted damaged area. The size of the damaged area should be determined based on economic thresholds related to the objective of the study or application. It is most probable that spectral identification of TSSM damage would be specific for crop or even development stage of the crop, since these factors have an influence on the spectral reflectance of leaves.

Table 7 – Cross-validation of the PLS-DA classification model of four damage levels based on the hyperspectral and multispectral reflectance of the bean leaves. The hyperspectral model is the result of three latent variables, and the multispectral model is of four latent variables.

	No damage	Low damage	Medium damage	High damage	Total predicted as	User accuracy % correct
Hyperspectral reflectance						
Confidence limit of ±4.5% for the overall accuracy, and Kappa = 0.92						
No damage	**22**	0	1	0	23	95.7
Low damage	1	**26**	2	0	29	89.7
Medium damage	0	1	**24**	1	26	92.3
High damage	0	0	0	**26**	26	100
Total actual class	23	27	27	27	104	
Producer accuracy % correct	95.7	96.3	88.9	96.3		**94.2**
Multispectral reflectance						
Confidence interval of ±9.1% for the overall accuracy, and Kappa = 0.56						
No damage	**11**	4	3	0	18	61.1
Low damage	8	**16**	6	0	30	53.3
Medium damage	4	7	**16**	0	27	59.3
High damage	0	0	2	**27**	29	93.1
Total actual class	23	27	27	27	104	
Producer accuracy % correct	47.8	59.3	59.3	100		**67.3**

The bold values in the diagonal are the actual number of samples correctly classified and the bold value at the lower right corner of each sub table is the total accuracy in percentage.

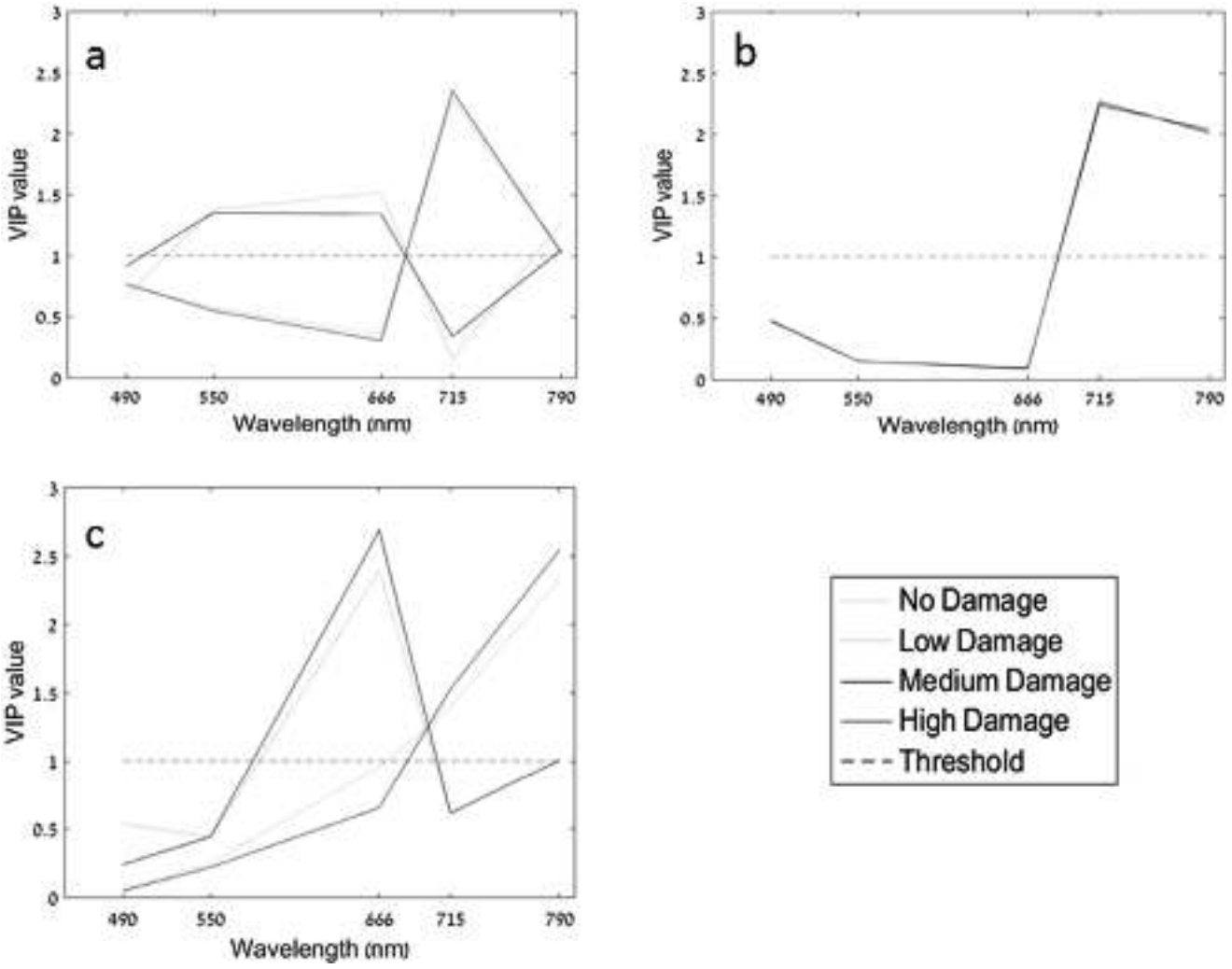

Fig. 7 – The variable importance in projection (VIP) values for the multispectral PLS-DA models obtained for pepper leaves: (a) reflectance; (b) absorbance; and (c) transmittance.

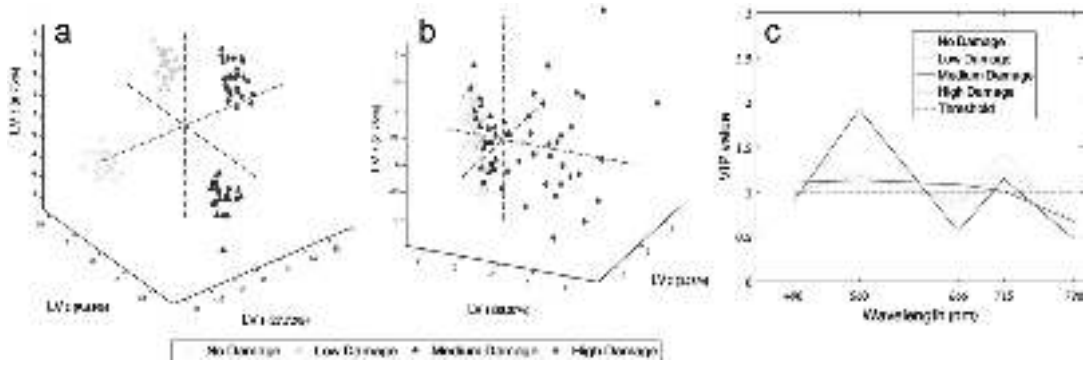

Fig. 8 – PLS-DA cross-validation results for bean leaves. Scores of the PLS-DA cross-validation multispectral models in three latent variables (LVs): (a) hyperspectral model and (b) multispectral model. (c) The variable importance in projection (VIP) values for the multispectral PLS-DA model.

3.3. *Two spotted spider mite spectral damage identification – site specific approach*

Arthropods damage can look similar to the chlorosis that results from abiotic stress. Stressed or damaged plants can be identified using spectral means. Spectrally identifying the type of stress is not an easy task, mainly since leaves stressed by different causes might appear spectrally similar. Chlorosis distribution on leaves can be related to the cause of the stress. Potassium deficiency begins on the leaf margins, while nitrogen deficiency begins more in the leaf centre, both resulting in discolouration. TSSM damage appears more in the leaf centre in spots with no relationship to veins (Fig. 1). Water stress is also needs to be considered as it can be spectrally assessed by reflectance measurements.

There is a wide range of available sensing devices, measuring techniques and spatial resolutions (Mahlein, Oerke, Steiner, & Dehne, 2012). Spectral identification analysis of TSSM damage to leaf, among other damages and stresses, has not yet been published. Therefore, in order to consider greenhouses as well as fields, site-specific applications that can distinguish early TSSM damage from other stresses are required and there is a need to consider the distribution of damage on the leaf. Proximal remote sensing, as reviewed by Nansen (2016), is in the forefront of pest management research.

As presented here, five spectral bands are enough to detect TSSM-damaged leaves. Therefore, utilising either a hyper- or multispectral high spatial resolution cameras in a greenhouse or field can enable damage or stress detection as an early stage. This can allow the image of the damaged or stressed leaves to be sent to pest experts and agronomists to evaluate and manage the problem. The next stage would be to analyse the spectral and spatial information of the damage or stress to assess its severity and/or cause. Since images can be accompanied by their location information, the exact location of the damaged or stressed leaves in the greenhouse or field would be known; therefore, treatments could be site specifically applied. Mirik et al. (2006) recommended digital imaging (i.e., using R, G and B bands) as an alternative to visual techniques of damage estimation, and Lucieer, Malenovsky, Veness, and Wallace (2014) showed that sub-leaf spatial resolution from the air has been available for some time. Iori et al. (2015) reported hyperspectral imaging at a sub-leaf resolution for disease detection in wheat at the ground level. Therefore, it is reasonable to assume that sub-leaf spatial resolutions could be also obtained by hyperspectral sensors mounted on low-flying drones.

4. Conclusions

In this study, greenhouse pepper and bean leaves were spectrally measured using sub-leaf resolution, in order to provide early TSSM damage detection. It was concluded that:

- GNDVI, NRENDVI, REIP, and TGI can separate between ND and the pepper leaves with TSSM damage, therefore allowing early TSSM damage identification. As a result of band availability in multispectral cameras, the preferable index was TGI; the second choice was GNDVI; and NRENDVI and REIP are the third choice.
- NDVI was the only VI that can separate the four damage levels obtained from bean leaves. The REBNDVI was an additional VI that can separate between ND and the rest of the damage levels obtained from bean leaves. Based on the availability in multispectral cameras, the preferable index was NDVI.
- Although the TSSM activity occurs on the underside of leaves, the three measuring methods (i.e., reflectance, absorbance and transmittance) resulted in similar qualities of early TSSM damage identification for VIs, as well as for the entire continuous spectrum. For the multispectral models, reflectance did not perform significantly better than the other two measuring methods. Therefore, reflectance, which is probably the only practical method for field and greenhouse applications, was assumed to be suitable for the task of early TSSM identification.
- PLS-DA hyperspectral models can identify early TSSM damage in greenhouse pepper or bean leaves when the sole damage is by TSSM.
- PLS-DA multispectral models can identify early TSSM damage in greenhouse pepper leaves when the sole damage is by TSSM.

- For reflectance measurements of bean leaves, PLS-DA hyperspectral model produced significantly better classification than the multispectral model, based on confidence limits as well as matrices comparison.
- For reflectance measurements of pepper leaves, PLS-DA hyperspectral model produced non-significant advantage over the multispectral model, based on confidence limits as well as matrices comparison.

As technology advances, the application of multispectral or hyperspectral analysis of image with sub-leaf spatial resolution for early TSSM damage identification holds potential for the future. The current study shows the potential of high spectral and spatial resolutions for TSSM damage detection.

Acknowledgement

This study was partially supported by Bio-Bee Biological Systems Ltd. Sde Eliyahu, Israel.

REFERENCES

Alatawi, F. J., Margolies, D. C., & Nechols, J. R. (2007). Aesthetic damage thresholds for twospotted spider mites (Acari : Tetranychidae) on impatiens: Effect of plant age and level of infestation. *Journal of Economic Entomology, 100*(6), 1904–1909.

Attia, S., Grissa, K. L., Lognay, G., Bitume, E., Hance, T., & Mailleux, A. C. (2013). A review of the major biological approaches to control the worldwide pest Tetranychus urticae (Acari: Tetranychidae) with special reference to natural pesticides. *Journal of Pest Science, 86*(3), 361–386. http://dx.doi.org/10.1007/s10340-013-0503-0.

Cohen, J. (1960). A coefficient of agreement for nominal scales. *Educational and Psychological Measurement, 20*(1), 37–46.

Cohen, Y., Alchanatis, V., Zusman, Y., Dar, Z., Bonfil, D., Karnieli, J., et al. (2010). Leaf nitrogen estimation in potato based on spectral data and on simulated bands of the VENuS satellite. *Precision Agriculture, 11*(5), 520–537. http://dx.doi.org/10.1007/s11119-009-9147-8.

Curran, P. J., Dungan, J. L., & Gholz, H. L. (1990). Exploring the relationship between reflectance red edge and chlorophyll content in slash pine. *Tree Physiology, 7*(1–4), 33–48.

Dekeyser, M. A. (2005). Acaricide mode of action. *Pest Management Science, 61*(2), 103–110. http://dx.doi.org/10.1002/ps.994.

Fitzgerald, G. J., Maas, S. J., & Detar, W. R. (2004). Spider mite detection and canopy component mapping in cotton using hyperspectral imagery and spectral mixture analysis. *Precision Agriculture, 5*(3), 275–289.

Foody, G. M. (2008). Harshness in image classification accuracy assessment. *International Journal of Remote Sensing, 29*(11), 3137–3158. http://dx.doi.org/10.1080/01431160701442120.

Fraulo, A. B., Cohen, M., & Liburd, O. E. (2009). Visible/near infrared reflectance (VNIR) spectroscopy for detecting twospotted spider mite (Acari: Tetranychidae) damage in strawberries. *Environmental Entomology, 38*(1), 137–142.

Gausman, H. (1985). *Plant leaf optical properties in visible and near infrared light*. Lubbock TX. USA: Texas Tech Press.

Gitelson, A. A., Kaufman, Y. J., & Merzlyak, M. N. (1996). Use of a green channel in remote sensing of global vegetation from EOS-MODIS. *Remote Sensing of Environment, 58*(3), 289–298.

Guyot, G., & Baret, F. (1988). Utilisation de la haute resolution spectrale pour suivre l'etat des couverts vegetaux. In *Paper presented at the 4th International Colloquium "Spectral signatures of objects in remote sensing", Aussois* (18–22 January).

Haboudane, D., Miller, J. R., Tremblay, N., Zarco-Tejada, P. J., & Dextraze, L. (2002). Integrated narrow-band vegetation indices for prediction of crop chlorophyll content for application to precision agriculture. *Remote Sensing of Environment, 81*(2–3), 416–426.

Herrmann, I., Berenstein, M., Paz-Kagan, T., Sade, A., & Karnieli, A. (2015). Early detection of two-spotted spider mite damage to pepper leaves by spectral means. In *The 10th European conference on precision agriculture, Volcani Center, Israel* (pp. 661–666).

Herrmann, I., Berenstein, M., Sade, A., Karnieli, A., Bonfil, D. J., & Weintraub, P. G. (2012). Spectral monitoring of two-spotted spider mite damage to pepper leaves. *Remote Sensing Letters, 3*(4), 277–283. http://dx.doi.org/10.1080/01431161.2011.576709.

Herrmann, I., Shapira, U., Kinast, S., Karnieli, A., & Bonfil, D. J. (2013). Ground-level hyperspectral imagery for detecting weeds in wheat fields. *Precision Agriculture, 14*(6), 637–659. http://dx.doi.org/10.1007/s11119-013-9321-x.

Hunt, E. R., Jr., Daughtry, C. S. T., Eitel, J. U. H., & Long, D. S. (2011). Remote sensing leaf chlorophyll content using a visible band index. *Agronomy Journal, 103*(4), 1090–1099. http://dx.doi.org/10.2134/agronj2010.0395.

Hunt, E. R., Jr., Hively, W. D., Fujikawa, S. J., Linden, D. S., Daughtry, C. S. T., & McCarty, G. W. (2010). Acquisition of NIR-green-blue digital photographs from unmanned aircraft for crop monitoring. *Remote Sensing, 2*(1), 290–305. http://dx.doi.org/10.3390/rs2010290.

Iori, A., Scala, V., Cesare, D., Pinzari, F., D'Egidio, M. G., Fanelli, C., et al. (2015). Hyperspectral and molecular analysis of *Stagonospora nodorum* blotch disease in durum wheat. *European Journal of Plant Pathology, 141*(4), 689–702. http://dx.doi.org/10.1007/s10658-014-0571-x.

Jacquemoud, S., & Baret, F. (1990). PROSPECT – a model of leaf optical-properties spectra. *Remote Sensing of Environment, 34*(2), 75–91. http://dx.doi.org/10.1016/0034-4257(90)90100-z.

Kant, M. (2006). *The consequences of herbivore variability for direct and indirect defenses of plants*. PhD. Amsterdam: University of Amsterdam. Retrieved from http://dare.uva.nl/record/1/255690.

Karnieli, A., Bayarjargal, Y., Bayasgalan, M., Mandakh, B., Dugarjav, C., Burgheimer, J., et al. (2013). Do vegetation indices provide a reliable indication of vegetation degradation? A case study in the Mongolian pastures. *International Journal of Remote Sensing, 34*(17), 6243–6262. http://dx.doi.org/10.1080/01431161.2013.793865.

Karnieli, A., Shachak, M., Tsoar, H., Zaady, E., Kaufman, Y., Danin, A., et al. (1996). The effect of microphytes on the spectral reflectance of vegetation in semiarid regions. *Remote Sensing of Environment, 57*, 88–96.

Kiang, N. Y., Siefert, J., Govindjee, & Blankenship, R. E. (2007). Spectral signatures of photosynthesis. I. Review of Earth organisms. *Astrobiology, 7*(1), 222–251. http://dx.doi.org/10.1089/ast.2006.0105.

Kumar, D., Raghuraman, M., & Singh, J. (2015). Population dynamics of spider mite, *Tetranychus urticae* Koch on okra in relation to abiotic factors of Varanasi region. *Journal of Agrometeorology, 17*(1), 102–106.

Lan, Y., Zhang, H., Hoffmann, W. C., & Lopez, J. J. D. (2013). Spectral response of spider mite infested cotton: Mite density and miticide rate study. *International Journal of Agricultural and Biological Engineering, 6*(1), 48–52. http://dx.doi.org/10.3965/j.ijabe.20130601.004.

Legowski, T. J. (1966). Experiments on predator control of glasshouse red spider mite on cucumbers. *Plant Pathology, 15*(1), 34–41.

Lucieer, A., Malenovsky, Z., Veness, T., & Wallace, L. (2014). HyperUAS-imaging spectroscopy from a multirotor

unmanned aircraft system. *Journal of Field Robotics, 31*(4), 571–590. http://dx.doi.org/10.1002/rob.21508.

Mahlein, A.-K., Oerke, E.-C., Steiner, U., & Dehne, H.-W. (2012). Recent advances in sensing plant diseases for precision crop protection. *European Journal of Plant Pathology, 133*(1), 197–209. http://dx.doi.org/10.1007/s10658-011-9878-z.

Migeon, A., & Dorkeld, F. (2015). *Spider mites web: A comprehensive database for the Tetranychidae*. Retrieved November 18, 2015, from http://www1.montpellier.inra.fr/CBGP/spmweb/notespecies.php?id=872#hosts.

Mirik, A., Michels, G. J., Kassymzhanova-Mirik, S., Elliott, N. C., Catana, V., Jones, D. B., et al. (2006). Using digital image analysis and spectral reflectance data to quantify damage by greenbug (Hemitera : Aphididae) in winter wheat. *Computers and Electronics in Agriculture, 51*(1–2), 86–98. http://dx.doi.org/10.1016/j.compag.2005.11.004.

Musumarra, G., Barresi, V., Condorelli, D. F., Fortuna, C. G., & Scire, S. (2004). Potentialities of multivariate approaches in genome-based cancer research: Identification of candidate genes for new diagnostics by PLS discriminant analysis. *Journal of Chemometrics, 18*(3–4), 125–132. http://dx.doi.org/10.1002/cem.846.

Mutanga, O., & Skidmore, A. K. (2007). Red edge shift and biochemical content in grass canopies. *Isprs Journal of Photogrammetry and Remote Sensing, 62*(1), 34–42.

Nansen, C. (2016). The potential and prospects of proximal remote sensing of arthropod pests. *Pest Management Science, 72*(4), 653–659. http://dx.doi.org/10.1002/ps.4209.

Nansen, C., Sidumo, A. J., Martini, X., Stefanova, K., & Roberts, J. D. (2013). Reflectance-based assessment of spider mite "bio-response" to maize leaves and plant potassium content in different irrigation regimes. *Computers and Electronics in Agriculture, 97*, 21–26. http://dx.doi.org/10.1016/j.compag.2013.06.007.

Navalon, A., Blanc, R., del Olmo, M., & Vilchez, J. L. (1999). Simultaneous determination of naproxen, salicylic acid and acetylsalicylic acid by spectrofluorimetry using partial least-squares (PLS) multivariate calibration. *Talanta, 48*(2), 469–475. http://dx.doi.org/10.1016/s0039-9140(98)00268-9.

Nihoul, P., Vanimpe, G., & Hance, T. (1991). Characterizing indices of damage to tomato by the two-spotted spider-mite, *Tetranychus urticae* koch [Acari, Tetranychidae] to achieve biological-control. *Journal of Horticultural Science, 66*(5), 643–648.

Paz-Kagan, T., Shachak, M., Zaady, E., & Karnieli, A. (2014). A spectral soil quality index (SSQI) for characterizing soil function in areas of changed land use. *Geoderma, 230*, 171–184. http://dx.doi.org/10.1016/j.geoderma.2014.04.003.

Raven, P. H., Everet, R. F., & Eichhorn, S. E. (2005). *Biology of plants* (7 ed.). New-York: W. H. Freeman and Company.

Reisig, D. D., & Godfrey, L. D. (2007). Spectral response of cotton aphid- (Homoptera : Aphididae) and spider mite- (Acari : Tetranychidae) infested cotton: Controlled studies. *Environmental Entomology, 36*(6), 1466–1474.

Reisig, D. D., & Godfrey, L. D. (2010). Remotely sensing arthropod and nutrient stressed plants- a case study with nitrogen and cotton aphid (Homoptera Aphididae). *Environmental Entomology, 39*(4), 1255–1263.

Rouse, J. W., Haas, R. H., Schell, J. A., & Deering, D. W. (1973). Monitoring vegetation systems in the Great Plains with ERTS. In *Third Earth Resources Technology Satellite -1 Symposium* (Vol. 1, pp. 309–317). Green-belt, MD, USA: NASA/GSFC.

Rozenstein, O., Paz-Kagan, T., Salbach, C., & Karnieli, A. (2015). Comparing the effect of pre-processing transformations on methods of land-use classification derived from spectral soil measurements. *IEEE Journal of Selected Topics in Applied Earth Observations and Remote Sensing, 8*(6), 2393–2404. http://ieeexplore.ieee.org/stamp/stamp.jsp?tp=&arnumber=6991564.

Sakai, Y., & Osakabe, M. (2010). Spectrum-specific damage and solar ultraviolet radiation avoidance in the two-spotted spider mite. *Photochemistry and Photobiology, 86*(4), 925–932. http://dx.doi.org/10.1111/j.1751-1097.2010.00739.x.

Tucker, C. J. (1979). Red and photographic infrared linear combinations for monitoring vegetation. *Remote Sensing of Environment, 8*(2), 127–150.

Wold, S., Johansson, E., & Cocchi, M. (1993). PLS – partial least squares projections to latent structures. In H. Kubinyi (Ed.), *3D QSAR in drug design: Theory, methods, and applications* (pp. 523–550). Leiden: ESCOM.

Yang, Z., Rao, M. N., Elliott, N. C., Kindler, S. D., & Popham, T. W. (2009). Differentiating stress induced by Greenbugs and Russian wheat aphids in wheat using remote sensing. *Computers and Electronics in Agriculture, 67*(1–2), 64–70. http://dx.doi.org/10.1016/j.compag.2009.03.003.

Yoder, B. J., & Pettigrew-Crosby, R. E. (1995). Predicting nitrogen and chlorophyll content and concentrations from reflectance spectra (400-2500nm) at leaf and canopy scales. *Remote Sensing of Environment, 53*(3), 199–211.

Zhao, J., Huang, L., Huang, W., Zhang, D., Yuan, L., Zhang, J., et al. (2014). Hyperspectral measurements of severity of stripe rust on individual wheat leaves. *European Journal of Plant Pathology, 139*(2), 401–411. http://dx.doi.org/10.1007/s10658-014-0397-6.